Robotica (1998) volume 16, pp. 551–563. Printed in the United Kingdom © 1998 Cambridge University Press

Analysis and control of a force display system driven by parallel wire mechanism

Tetsuya Morizono, Kazuhiro Kurahashi and Sadao Kawamura

Department of Robotics, Faculty of Science and Engineering, Ritsumeikan University, 1-1-1, Noji-Higashi, Kasatsu, Shiga, 525-0058 (Japan)
E-mail: gr010952@bkc.ritsumei.ac.jp, kawamura@bkc.ritsumei.ac.jp

(Received in Final Form: November 17, 1997)

SUMMARY
In this paper, we develop a force display system using parallel wire mechanism for virtual sports training with high speed motion. We firstly point out a control issue of the force display system driven by parallel wire mechanism. Based on the analysis, control laws are proposed to improve performance of the force display system. It is experimentally demonstrated that the proposed control laws realize higher acceleration and lower reaction force than other force display systems. Using the experimental result, the performance of the system is evaluated quantitatively.

KEYWORDS: Force display system; Parallel wire mechanism; Structural transparency; Elasticity; Feedback control law; Stability analysis; Performance evaluation.

1. INTRODUCTION

Visual display systems are widely utilized in virtual reality to provide information for human operators. Since humans obtain most of the information through visual sensation, it is natural that many visual display systems are developed. Recently, new types of display systems such as an HMD (Head Mounted Display) are proposed.[1,2]

However, when human operators mechanically interact with an object in the virtual world, using only the visual display system is not enough to obtain good quality of virtual reality. In such a situation, it is better to display force sensation of a virtual object to humans in addition to visual sensation. In the near future, virtual reality will be applied to many fields such as sports training, rehabilitation etc. In these applications, the system displaying the force sensation, namely the *force display system* is essential.

In this paper, we focus on sports training as an application of virtual reality. A force display system that satisfies the following characteristics is proposed for this application:

(i) A large motion area not to restrict motion range of operators,
(ii) High speed motion capacity not to impede motion of operators,
(iii) Operator's safety, and
(iv) Structural Transparency.[3]

Here, the structural transparency is the concept that human operators ideally feel zero reaction force from the force display system if the desired force is set as zero. In practice, however, there are reaction forces due to dynamic characteristics of the force display system.

From a mechanical viewpoint, we discuss how to realize the force display system which satisfies the above four characteristics. Although some force display systems have been proposed, it is difficult to realize these four characteristics simultaneously. This is because the first and the second characteristics conflict with the third and the fourth ones.

One way to realize a large motion area is to adopt a *serial link mechanism*.[4,5] This system is often used as a master arm in a master–slave system (for example, refs 6–8). However, this mechanism inherently has a dynamic characteristic of large mass/inertia. This characteristic brings the force display system a trade-off between the high speed motion capacity and the human's safety.

Parallel *link* mechanism is often used in the haptic device to decrease its apparent mass/inertia.[9–13] However, it is noted that the haptic device is generally designed to be compact, namely to have a small motion area with a small mechansm. To realize a force display system with a larger motion area, a larger mechanism is needed. For such a mechanism, we cannot avoid increase of its mass/inertia. As a result, it is predicted that similar problems to those in the serial link type of system will arise using this system.

To overcome the difficulty of satisfying the four characteristics, we propose a force display system using a *parallel wire mechanism* as seen in Figures 1 and 2. This mechanism has some mechanical advantages as follows:

Low apparent mass/inertia: By using this mechanism, we can equip the force display system with a grip handle of low mass/inertia. The grip handle is actuated by wires. Due to low mass/inertia of the mechanism, we can utilize low-powered actuators to obtain high speed motion capacity.
Simple structure: Since wires are used directly to transmit the generated torque/force at the actuator unit to the grip handle, we do not need complicated mechanical parts for the transmission of the torque/force.
Large motion areas: We need only longer wires to realize a larger motion area. Even in such a system, low mass/inertia is guaranteed because the mass of the wire is small.

These advantages contribute a large motion area, high speed motion capacity and operator's safety to a force display system. In fact, in literature of manipulators' design using this mechanism, *FALCON* has demonstrated the high

https://doi.org/10.1017/S0263574798000551 Published online by Cambridge University Press

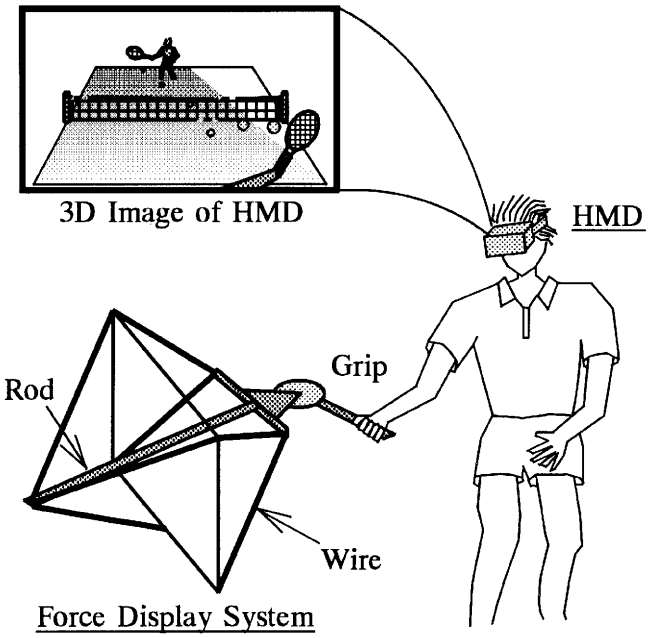


Fig. 1. Conceptual sketch of virtual tennis system.

speed motion capacity of this mechanism.[14]

In literature of the *force display system driven by parallel wire mechanism*, Sato et al. propose a system called *SPIDAR*.[15,16] The effectiveness of using the force display system when human operators interact with a virtual object is reported. Kawamura and Ito propose a master robot using this mechanism for a master-slave system.[17] There, a principle of *minimum numbers of wires* is derived based on a concept of the *vector closure*.[18] Recently, a system called *WireMan* is also proposed.[19] However, the previous studies have not discussed the four requirements to the force display system for virtual sports. Moreover, these studies have not quantitatively evaluated performance of the system using parallel wire mechanism. Therefore, we need detail analysis on the parallel wire mechanism through a simple model. In addition, some control laws are proposed based on the dynamic characteristics of the parallel wire mechanism.

In this paper, we will first investigate the dynamic charactristic of the parallel wire mechanism through a simple model. In addition, some control laws are proposed based on the dynamic characteristics of the parallel wire mechanism.



Fig. 2. Realized virtual tennis system.

The remainder of this paper is organised as follows: In Section 2, we introduce the virtual tennis system as an application of the force display system driven by parallel wire mechansim. In Section 3, we propose an analysis model of the system, where we take account of elastic elements from the wires and other mechanical parts. Discussion for the model of the elastic elements of the system is given in Section 4. In Section 5, we derive the dynamics of the system and present coefficients of the dynamics. In Section 6, we theoretically point out control issues of the force display system driven by parallel wire mechanism. From the theoretical analysis, we propose control laws based on the feedback approach in Sections 7 and 8. In Section 9, effectiveness of the proposed control laws is demonstrated through basic exprimental results. We also give a quantitative evaluation of the system in this section. Finally, conclusion is given in Section 10.

2. AN EXAMPLE OF FORCE DISPLAY SYSTEM DRIVEN BY PARALLEL WIRE MECHANISM

As an example of virtual reality of the force display system driven by parallel wire mechanism, we consider the *virtual tennis system* in this section.[20] A conceptual sketch of the system is shown in Figure 1. Since it is difficult to realise all motions of *real* tennis in the virtual world, we assume that

- an operator (player) stays around a certain point in virtual tennis court, and
- the operator hits a virtual ball with a forehand or backhand swing.

As shown in Figure 1, the virutal tennis system has two displays: an HMD (Head Mounted Display) and the force display system driven by parallel wire mechanism. Under the above assumption, the goal of the virtual tennis system is described as follows:

- Through the HMD, the operator can see a virtual tennis field such as a virtual ball, a virtual racket, a virtual court etc.
- Through the force display system, the operator can feel mass/inertia of the virtual racket, and a reaction force when the operator hits the virtual ball with the virtual racket.

The realized virtual tennis system is shown in Figure 2, and the diagram of the control system is shown in Figure 3. On the HMD, there are three gyro sensors to measure an orientation of the operator's head. The signal of the orientation is sent to two PCs (Personal Computers) via DSP (Digital Signal Processor). Based on this signal, each PC generates an image of the virtual tennis field, and sends it to each LCD (Liquid Crystal Display) in the HMD. Since two image (for both eyes of the operator) are generated with some disparity, the operator can see a 3-dimensional view in the HMD.

The force display system driven by parallel wire mechanism is controlled with the DSP. In the wires of the system, tension sensors using strain gages are installed. The signals of the sensors are sent to the DSP via strain

https://doi.org/10.1017/S0263574798000551 Published online by Cambridge University Press

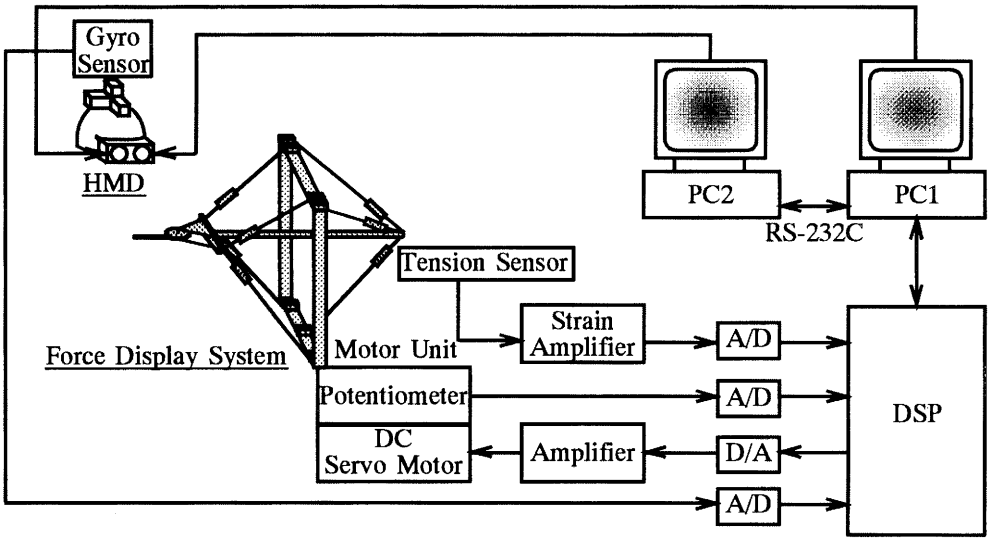


Fig. 3. Diagram of control of virtual tennis system.

amplifiers and 12-bits A/D converters built in the DSP. Using the tension signals and the position signal of the grip handle, the DSP implements a control law of the force display system. In ref. 20, only basic experimental results were demonstrated. Therefore, the dynamic charactristic and stability were not clear. We will discuss these issues in the following sections.

3. EXPERIMENTAL SYSTEM WITH 1 D.O.F.

To simplify the explanation, we deal with a 1 D.O.F. force display system driven by two wires. However, the following discussion can be applied to a general *n* D.O.F. system.

3.1 Components

The 1 D.O.F. system driven by two wires is shown in Figure 4. This system consists of

- two motor units,
- a base frame to attach the motor units,
- two wires and two tension sensors,
- a grip handle, and
- guide rails to constrain the other 5 D.O.F. motions of the grip handle.

The designed motion length is approximate 1.6 [m]. This system is placed vertically. The handle can be moved up and down in the vertical direction along the guide rails, and can give an operator a force in this direction. We use four guide rollers between the grip handle and the guide rails to reduce the influence of the static and the coulomb frictional forces.

The motor unit shown in Figure 5 is used to actuate a wire and to measure a length of the wire. Its basic strcutrue is depicted in Figure 6. A 60 [W] DC servomotor (actuator) generates a torque to drive a wire. This torque is transmitted to a wire drive pulley via a reduction mechanism using two timing belts. The reduction ratio is 10.3. The actuating torque is transformed to the tension at the wires. A potentiometer is connectd to the same axis of the wire drive pulley in order to measure the length of the wire as a rotating angle of the potentiometer.

The grip handle of this system is shown in Figure 7. The base of the handle is a steel plate, whose size is 100×100 [mm] and 6 [mm] thick. On the base plate, a small aluminum plate is attached as a grip for the operator. By measuring the strain of the grip using two strain gages, we obtain the operational force which the operator exerts on the grip handle as well as each wire tension.

3.2 Model

A model for analysis of the system is shown in Figure 8. In this model, the motor unit which is originally a rotational

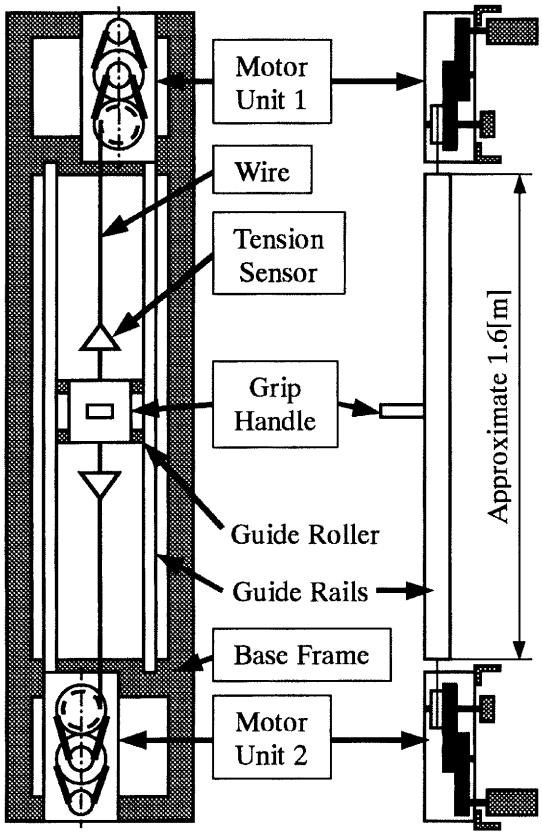


Fig. 4. 1-D.O.F. force display system driven by two wires.

https://doi.org/10.1017/S0263574798000551 Published online by Cambridge University Press

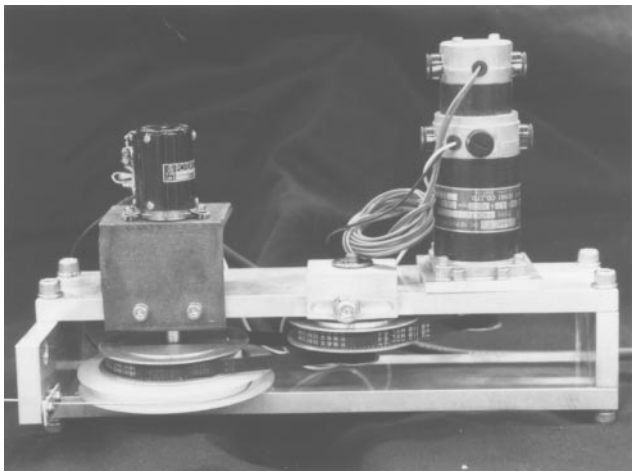


Fig. 5. Motor unit.

type is expressed as a linear equivalent one. The grip handle is assumed to be a point mass.

In the following discusson, we assume that the actuator has enough capacity not to loosen the wire. Static and coulomb frictional forces are not taken into account in the model. We do not consider the gravity term explicitly by compensating it.

Notations in Figure 8 are defined as:

J: An equivalent inertial coefficient of the motor units, which includes those of both the actuator and the reduction mechanism,

D: An equivalent viscous coefficient of the motor units, which includes those of both the actuator and the reduction mechanism,

m and d: An inertial and a viscous coefficients of the grip handle,

x_i: A position of the equivalent inertia of the ith motor unit ($i=1, 2$),

x: A position of the grip handle,

f_i: A tension of the ith wire connnected to the ith motor unit,

f_{di}: A desired wire tension of the ith wire,

τ_i: An input torque for the ith motor unit,

f_{dh}: A desired reaction force for an operator, and

f_h: An operational force which the operator exerts on the grip handle.

Note that positive directions of τ_2 and f_2 are opposite to those of τ_1 and f_1 respectively.

In the case of the 1 D.O.F. system driven by two wires, the desired wire tension f_{di} ($i=1, 2$) is related with the desired reaction force f_{dh} as follows:

$$f_{dh}=f_{d1}-f_{d2}. \tag{1}$$

Using only equation (1), the desired wire tensions cannot be uniquely determined from a given f_{dh}. However, by setting the *minimum wire tension* not to loosen the wire f_0 to the desired wire tensions f_{di} ($i=1, 2$) in advance, these tensions are uniquely determined. Here, f_0 is a positive constant.

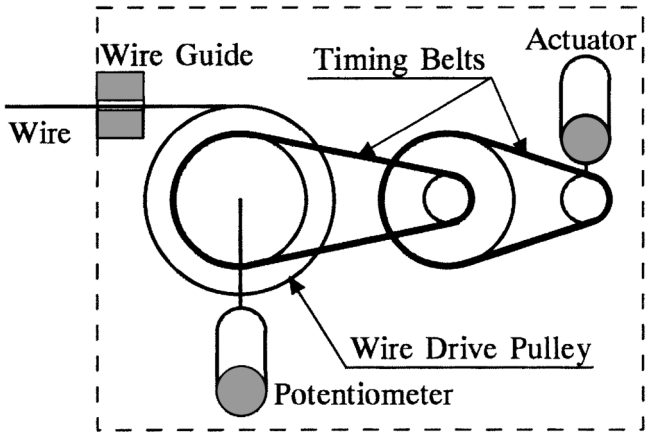


Fig. 6. Structure of motor unit.

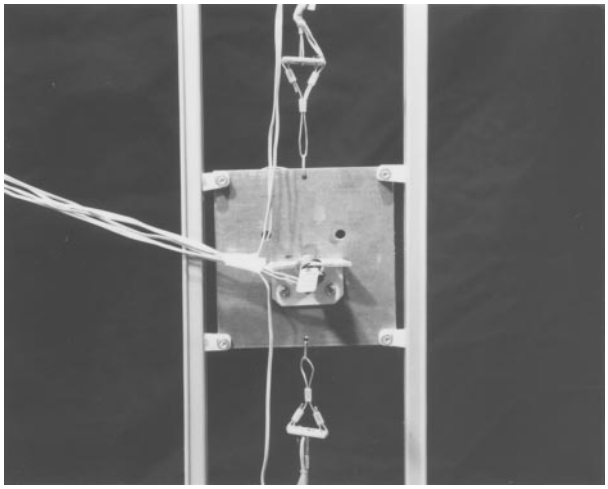


Fig. 7. Grip handle.

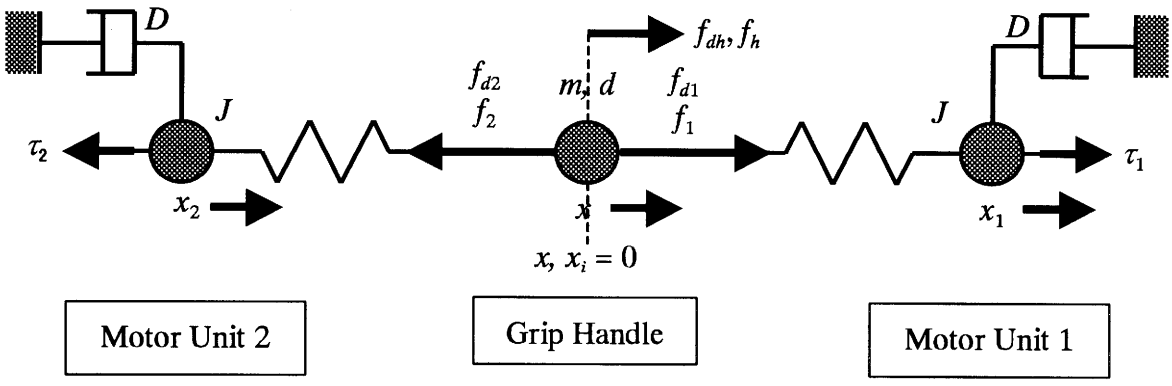


Fig. 8. Model of 1 D.O.F. force display system.

https://doi.org/10.1017/S0263574798000551 Published online by Cambridge University Press

In the model, we suppose that the grip handle and both motor units are connected by two springs. Each spring expresses elastic elements of the system from wires, tension sensors, timing belts etc.

4. MODEL OF SPRING ELEMENT

4.1 Tensile property of motor unit and wire

To complete the model of the sysem presented in Section 3, the model of the spring is needed. Therefore, we investigated tensile property of the motor unit and the wire through a basic experiment.

4.1.1 Experimental setup. The experimental setup is shown in Figure 9. In this experiment, the motor unit is mounted on the upper side of a rigid frame, and the end of the wire is connected to the lower side of that frame. Moreover, a laser ranger is hung from the upper side of the frame with a rigid rod to measure bends of both sides of the frame. Note that a rotary encoder which is connected to the same axis with the DC servomotor (*not* to the axis of the wire drive pulley) is used in this experiment. By setting the encoder in this way, we can measure the characteristic of the spring element including the elasticity of the reduction mechanism.

A tension was then given to the wire by driving the motor unit, and a rotational displacement of the DC servomotor was measured. This displacement was transformed to the equivalent linear one, corresponding to the spring model shown in Figure 8. In this experiment, we firstly increased the wire tension up to 50 [N]. The rotational angle of the DC servomotor and the tension were measured at the interval of 5 [N]. The tension was kept constant during the measurement. We increased 5 [N] of the tension for approximately 5 [s] so that the dynamics of the motor unit did not affect the experimental results. In the same manner, we decreased the wire tension to 0 [N] again after it reached 50 [N].

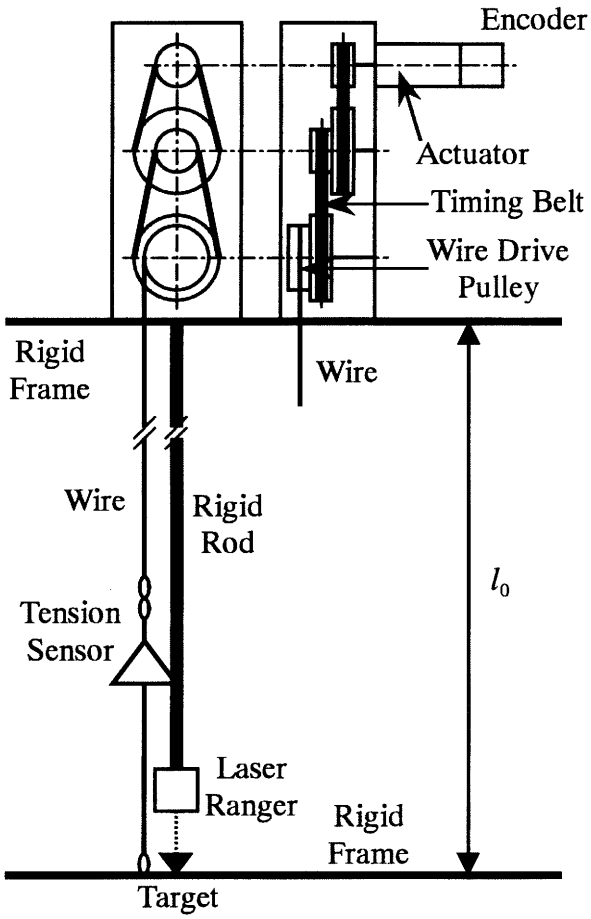


Fig. 9. Experimental setup to examine spring elements.

4.1.2 Experimental results. Experimental results are shown in Figure 10. The ordinate denotes the tension f_i and the abscissa denotes the corresponding equivalent displacement Δx. Here, since the bend of the frame was less than 50 [μm] and much smaller than the range of the displacement shown in Figure 10, we ignore the bend. The parameter l_0 in Figures 9 and 10 denotes the basic wire length when the wire is not tensed. In this experiment, we changed l_0 to 500, 1000 and 1500 [mm].

From Figure 10, we observe that

- the tensile property of the motor unit and the wire varies accoding to the basic wire length l_0,
- the tensile property has hysteresis, and
- the tension f_i is nonlinearly proportional to the displacement Δx of the spring.

4.2 Assumption and its validity

4.2.1 Assumption on tension. Before operating the system, the wires (including the tension sensors and the reduction mechanisms) are tensed by the internal forces and their displacements become $x_1 - x = a$ and $x - x_2 = a$ (or $x_2 - x = -a$), where a denotes the initial displacement of the wires and is a positive constant.

The tension property shown in Figure 10 is observed only with elongation. Therefore, the relation between force and displacement does not hold when the wire shrinks. To

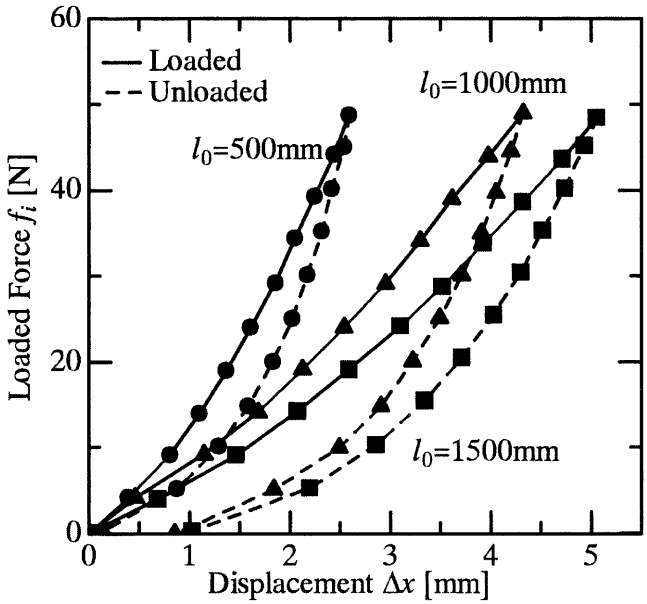


Fig. 10. Tensile property of motor unit.

https://doi.org/10.1017/S0263574798000551 Published online by Cambridge University Press

simplify analysis on the parallel wire mechanism, we make the following assumption:

Assumption on tension: During the motion exerted by operators, the tensions f_1 and f_2 are kept positive or the differences $x_1 - x$ and $x - x_2$ are kept positive.

The above assumption means that even though the operator moves the grip handle quickly, wire tensions f_1 and f_2 are always kept positive, or the wires do not loosen. In practice, it is impossible to satisfy the assumption for all frequency of the operator's motion because of the delay in force feedback. However, the above assumption will hold for low frequency. The validity of the assumption is checked by the following experiment.

4.2.2 Experimental setup. In this experiment, we used the 1 D.O.F. force display system. The desired reaction force f_{dh} for the operator was set as $f_{dh}=0$. The operator oscillated the grip handle with some frequencies. During operaton, we measured the position of the grip handle x by a laser ranger and that of each equivalent inertia of each motor unit x_i $(i=1, 2)$ by an incremental encoder as a rotational angle of the DC servomotor. Displacements of wires $x_1 - x$ and $x - x_2$ were obtained from these positions. The system employed the tension and reaction force feedback law (the control law will be discussed in Section 8). The minimum wire tension was 19.6 [N].

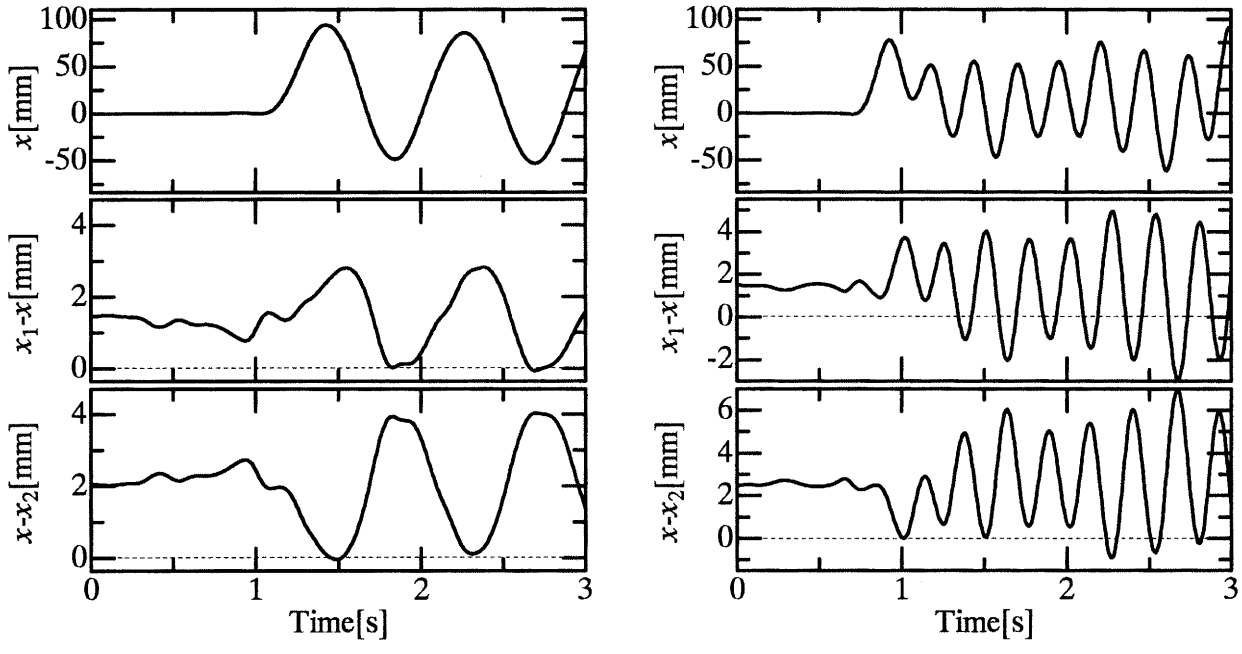
4.2.3 Experimental results. Two results are shown in Figure 11. In Figure 11(a), frequency and amplitude of the grip handle motion are approximate as 1 [Hz] and 70 [mm] respectively. In Figure 11(b), they are approximate as 4 [Hz] and 58 [mm]. Since the operator freely oscillated the grip handle, exact frequency and amplitude were not obtained. Here, $x=0$ denotes the middle point between both motor units.

In Figure 11, we observe that before the grip handle was oscillated, the displacement of each wire were held to be constant by the internal force. We regard this displacement as an inital one a. Here, the initial displacement of $x_1 - x$ is different from that of $x - x_2$. It is presumed that such difference is caused from the error when we initialize the incremental encoder at $x_1=0$.

From the experimental results in Figure 11(b), we see that the system cannot satisfy the assumption when the grip handle is oscillated. This is because most of minimum values are negative. In contrast, the assumption is satisfied in the experimental result shown in Figure 11(a), where the grip handle is oscillated with frequency 1 [Hz] and amplitude 70 [mm].

4.3 Discussion on model of spring element

Under the assumption, we discuss the model of the spring shown in Figure 8. We firstly consider dependence of the tensile property on the wire length. The elastic characteristic of the system varies when the grip handle is moved, because the length of the wire is changed according to the position of the grip handle. However, note that the parallel wire mechanism is generally designed so that its *feasible* (theoretical) motion area is larger than the motion area which is actually used. In this case, since variation of the wire length becomes relatively small, the elastic characteristic of the system varies within a certain bound. From this consideration, we treat the spring shown in Figure 8 as one with a constant characteristic in this paper. Since validity of the assumption was demonstrated around $x=0$ and the corresponding wire length when $x=0$ is approximate 800 [mm], we shall focus on the characteristic in the case



(a) Frequency 1[Hz] (b) Frequency 4[Hz]

Fig. 11. Experimental result to check validity of assumption.

https://doi.org/10.1017/S0263574798000551 Published online by Cambridge University Press

Table I. Spring constants estimated from tensile property

Wire length l_0	k_1 [N/mm]	k_2 [N/mm^2]
500 [mm]	6.219	4.160
1000 [mm]	6.544	1.110
1500 [mm]	4.968	0.9310

that the basic wire length l_0 is 1000 [mm].

Secondly, we consider hysteresis of the tensile property. As shown in Figure 11(a), the displacements $x_1 - x$ and $x - x_2$ remain positive, and are within 2.8 [mm] and 4.0 [mm] respectively. Each variation range of the displacement was smaller than that when the motor unit was examined (Figure 10). In such situation, influence of hysteresis on the tensile property will also be smaller. Therefore, we approximate the tensile property to the solid curve which means the characteristic when the motor unit is loaded.

Taking the above considerations into account, since the tension f_i is nonlinearly proportional to the displacement Δx in Figure 10, we express the model of the spring shown in Figure 8 as

$$f_i = k_1 \Delta x + k_2 \Delta x^2 \quad (i = 1, 2), \tag{2}$$

where k_1 and k_2 denote spring constants for the linear and quadratic terms respectively. Using the tensile property obtained through the experiment, we estimated k_1 and k_2 by the least square method for each basic wire length. The estimated spring constants are summarized in Table I. In this paper, we focus on the result in the case of the basic wire length $l_0 = 1000$ [mm], which has $k_1 = 6.544$ [N/mm] and $k_2 = 1.110$ [N/mm^2].

Substituting $x_1 - x$ and $x - x_2$ into Δx in equation (2), we have

$$f_1 = k_1(x_1 - x) + k_2(x_1 - x)^2, \tag{3}$$

$$f_2 = k_1(x - x_2) + k_2(x - x_2)^2. \tag{4}$$

When the assumption in Section 4.2 is valid, we can linearize equations (3) and (4) around $x_1 - x = a$ and $x - x_2 = a$. Applying Taylor's expansions to $(x_1 - x)^2$ and $(x - x_2)^2$ yields

$$(x_1 - x)^2 = a^2 + 2a(x_1 - x - a) = 2a(x_1 - x) - a^2, \tag{5}$$

$$(x - x_2)^2 = a^2 + 2a(x - x_2 - a) = 2a(x - x_2) - a^2. \tag{6}$$

Substituting equations (5) and (6) into equations (3) and (4), we obtain

$$f_1 = K_0(a)(x_1 - x) - k_2 a^2, \tag{7}$$

$$f_2 = K_0(a)(x - x_2) - k_2 a^2, \tag{8}$$

where $K_0(a)$ is defined as

$$K_0(a) \triangleq k_1 + 2k_2 a, \tag{9}$$

and denotes stiffness of the linearized spring. This constant is determined by the initial displacement a, and can be set large by increasing a.

5. DYNAMICS

Using the model as shown in Figure 8, derivation of the dynamics of the force display system is straightforward. We firstly obtain the dynamics of motor units as follows:

$$J\ddot{x}_1 + D\dot{x}_1 + f_1 = \tau_1, \tag{10}$$

$$J\ddot{x}_2 + D\dot{x}_2 - f_2 = -\tau_2. \tag{11}$$

On the other hand, the dynamics of the grip handle is expressed by

$$m\ddot{x} + d\dot{x} = f_1 - f_2 + f_h. \tag{12}$$

The models of the springs are given in equations (7) and (8). These five equations are related with the dynamics of the system.

Noting that

$$-f_2 = K_0(a)(x_2 - x) + k_2 a^2, \tag{13}$$

substituting equations (7) and (13) into equations (10) through (12) yields

$$J\ddot{x}_1 + D\dot{x}_1 + K_0(x_1 - x) = \tau_1 + k_2 a^2, \tag{14}$$

$$J\ddot{x}_2 + D\dot{x}_2 + K_0(x_2 - x) = -\tau_2 - k_2 a^2, \tag{15}$$

$$m\ddot{x} + d\dot{x} = K_0(x_1 + x_2 - 2x) + f_h. \tag{16}$$

Applying Laplace transforms to equations (14) through (16), we obtain

$$(Js^2 + Ds + K_0)X_1 - K_0 X = T_1 + k_2 a^2/s, \tag{17}$$

$$(Js^2 + Ds + K_0)X_2 - K_0 X = -T_2 - k_2 a^2/s, \tag{18}$$

$$(ms^2 + ds + 2K_0)X = K_0(X_1 + X_2) + F_h, \tag{19}$$

where X, X_i $(i = 1, 2)$, T_i and F_h denote Laplace transforms of x, x_i, τ_i and f_h respectively. Then we eliminate X_1 and X_2 from equations (17) through (19) to obtain

$$\left\{\frac{Jm}{K_0}s^4 + \frac{Jd + Dm}{K_0}s^3 + \left(\frac{Dd}{K_0} + m + 2J\right)s^2 + (d + 2D)s\right\}X = T_1 - T_2 + \left(\frac{J}{K_0}s^2 + \frac{D}{K_0}s + 1\right)F_h. \tag{20}$$

Here, we consider the following feedback law to understand the dynamics of the system more clearly,

$$\tau_i = K_f(f_{di} - f_i) + f_{di} \quad \text{or} \quad T_i = K_f(F_{di} - F_i) + F_{di} \quad (i = 1, 2), \tag{21}$$

where F_{di} $(i = 1, 2)$ denote the Laplace transforms of f_{di}. We name the control law in equation (21) as the tension feedback law.

Substituting equation (21) for $i = 1, 2$ to equation (20) yields

$$N_K + \left\{\left(m + \frac{2J}{K}\right) + \left(d + \frac{2D}{K}\right)\right\}X = F_{dh} + F_h, \tag{22}$$

$$N_K = \frac{1}{K_0 K}[\{Jms^4 + (Jd + Dm)s^3 + Dds^2\}X - (Js^2 + Ds)F_h], \tag{23}$$

where $K = K_f + 1$ and

$$F_{dh} = F_{d1} - F_{d2}, \tag{24}$$

https://doi.org/10.1017/S0263574798000551 Published online by Cambridge University Press

Table II. Values of coefficients

Coefficient	Value
J [kg]	0.687
D [kg/s]	$22.32 < D < 45.14$
m [kg]	0.5
d [kg/s]	0
K_0 [N/m]	8764

denotes the Laplace transform of f_{dh}.

Table II presents the values of the following five coefficients: The inertial and viscous coefficients of the motor unit (J and D), those in the grip handle (m and d), and the spring constant K_0. The mass of the handle is obtained by actual measurement. Recall that static and coulomb frictional forces are not taken into account in this paper. In this case, the viscosity of the handle comes from that of the air. Since the viscosity due to the air is usually very small (within 10 [m/s] or 20 [m/s] movement of the handle), we assume that the viscous coefficient of the handle $d = 0$.

Taking account of the fact that the reduction ratio of the motor unit is over 10.0, and the wire drive pulley and the pulleys in the reduction mechanism are made of synthetic resin and duralumin repectively, we suppose that the inertia property of the motor unit is dominated by that of the DC servomotor. We calculated the inertial coefficient of the motor unit J based on the value of the inertia of the DC servomotor given in the catalogue.

The viscous coefficient D was estimated from an experimental result in Section 9.2 (detail of the experiment will be explained there). In this experiment, we obtained different values of the coefficient D for different minimum wire tensions. It is presumed that the difference comes from the estimation error. In this paper, we adopt 22.32 [kg/s] as the value of the coefficient D (the corresponding minimum wire tension f_0 is 24.5 [N]). However, it should be noted that the discussion in the following sections can be applied even if the coefficient D has a different value.

We calculated the stiffness K_0 in the following way: As discussed in Section 4, $k_1 = 6.544$ [N/mm] and $k_2 = 1.110$ [N/mm^2], which are the spring constants in the case that the basic wire length is 1000 [mm]. Next, we obtained the value of the initial displacement a from Figure 11(a). In this paper, the initial displacement was chosen as $a = 2.0$ [mm]. From definition of the stiffness K_0 in equation (9), K_0 was calculated as 8.764 [N/mm] or 8764 [N/m].

6. CONTROL ISSUE

In this section, we clarify the control issue of this system. As mentioned in Section 1, the force display system generally requires the structural transparency. In other words, it has to let an operator feel the desired reaction force even if the grip handle is in *any* motion. Therefore, the ideal condition of the structural transparency is described in frequency domain as

$$F_{dh} = -F_h \quad \text{or} \quad F_{dh} + F_h = 0. \tag{25}$$

Here, we should note that $-F_h$ denotes the reaction force which an operator actually feels. Comparing equation (25) to equation (22), we see that the entire left side of equation (22) degrades the structural transparency. For convenience, we let

$$F_\Delta = N_K + \left\{ \left(m + \frac{2J}{K} \right) s^2 + \left(d + \frac{2D}{K} \right) s \right\} X. \tag{26}$$

By observing F_Δ in detail, we understand that the F_Δ consists of two components. The first term N_K given by equation (23) includes higher order terms on X and F_h and is resulted from the elasticity of the system (that is, the spring shown in Figure 8). If the motor units and the grip handle are connected rigidly or K_0 tends to infinity, this term will disappear. The remainder of F_Δ is the dynamic element of the system which contains inertias and viscosities of the grip handle and both motor units.

Control laws should reduce the influence of F_Δ to improve the structural transparency. Keeping this in mind, we discuss the control laws based on the feedback approach. We will deal with this issue in two steps corresponding to the two components of F_Δ.

In Section 7, a method of reducing the influence of the elasticity is proposed for the tension feedback law. In Section 8, we propose a control law to suppress the effect of the dynamic element of the system. In addition, stability of the system is analyzed in both sections.

7. TENSION FEEDBACK LAW

Firstly, we consider the method of reducing the influence of the elasticity (namely, the term N_K shown by equation (23)) in the case of the tension feedback law.

7.1 High gain feedback

One possible method to reduce the influence of the term N_K in equation (26) is to modify the tension feedback law equation (21) so that it compensates the term N_K. However, such a control law would become complex in general and might require a higher order signal of the handle position x. Though such control law may not be impossible to implement, difficult problems could arise from a practical point of view.

Here, we focus on the structure of the term N_K shown in equation (23). This term is inversely proportional to K, namely the feedback gain K_f of the tension feedback law (note that $K = K_f + 1$). Therefore, we will be able to reduce the influence of the term N_K by increasing the magnitude of K_f. Such method of using high gain feedback seems to be practical because the tension feedback law is easy to implement. However, there is limitation of the feedback gain because of the stability problem. That is, there is a certain margin for the magnitude of the feedback gain to guarantee that the system remains stable. From this consideration, we investigate the stability of the system with respect to the magnitude of the feedback gain.

7.2 Stability analysis

Since we focus on the high speed motion capacity and the structural transparency of the system in this paper, we let

https://doi.org/10.1017/S0263574798000551 Published online by Cambridge University Press

$F_{dh}=0$ in equation (22). Then from this equation, we obtain the following transfer function G_{FX} from the operational force F_h to the handle position X,

$$G_{FX}=\frac{X}{F_h}=\frac{\frac{J}{K_0K}s^2+\frac{D}{K_0K}s+1}{\frac{Jm}{K_0K}s^4+\frac{Jd+Dm}{K_0K}s^3+\left(\frac{Dd}{K_0K}+m+\frac{2J}{K}\right)s^2+\left(d+\frac{2D}{K}\right)s}. \quad (27)$$

By substituting various values for K, we obtain a plot of poles and zeros of the transfer function equation (27) in a complex number plane. This plot is shown in Figure 12, in which K is increased from 1 to 250. Corresponding to equation (27), there are four poles and two zeros. One pole stays at the origin of the complex number plane independent of the values of K. In contrast, the other poles and zeros are dependent on the values of K. When the value of K is increased, two poles and two zeros will tend to infinity in the left half plane. However, the other one pole approaches the origin (namely, the imaginary axis). This means that the stability margin is decreased by increasing the feedback gain. As a result, we will not be able to set an excessively large value for the feedback gain. Moreover, we have to recall that in the model shown in Figure 8, some mechanical properties of the system such as static and coulomb frictonal forces, and nonlinearity and hysteresis of the spring have not been included. This "unmodeled" dynamics may be excited with the high gain feedback and drive the system to an unstable or oscillating situation. To avoid that, we should design the margin for stability of the system as large as possible.

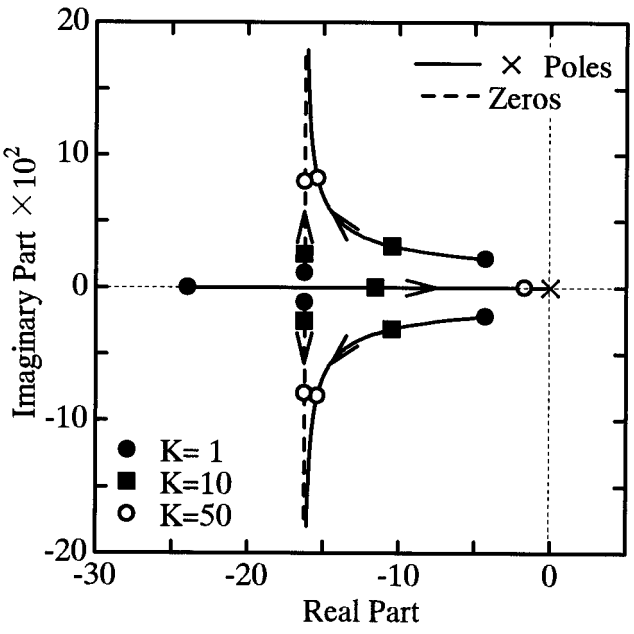


Fig. 12. Plot of poles and zeros of transfer function G_{FX}.

8. TENSION AND REACTION FORCE (T-RF) FEEDBACK LAW

8.1 Drawback of tension feedback law

Next, we focus on the remaining term of F_Δ minus N_K. This part can be regarded as the dynamic term of the system, including inertias and viscosities of the grip handle and both motor units. From the structure of the dynamic term as shown in equation (26), we understand that while the inertia and the viscosity of the motor units are dominated by K or the feedback gain K_f, those of the grip handle are not. Therefore, the method of increasing the feedback gain can also be applied to the motor units to reduce their dynamic effects. However the influence coming from the dynamics of the grip handle cannot be decreased.

Since the system in this paper aims at high speed motion capacity, it is better to reduce the dynamic effect of the grip handle from the viewpoint of the structural transparency. Based on this idea, we propose a method of reducing this effect.

8.2 Control law and its effect

We consider the following "modified" desired wire tensions,

$$\tilde{F}_{d1}=F_{d1}+\frac{1}{2}(ms^2+ds)X, \quad (28)$$

$$\tilde{F}_{d2}=F_{d2}-\frac{1}{2}(ms^2+ds)X. \quad (29)$$

Clearly, the above modified desired wire tensions consist of two parts, that is,

(The component for the desired reaction force f_{dh})

$+\frac{1}{2}$(The dynamic terms of the grip handle).

In other words, the modified desired wire tensions $\tilde{F}_{di}\,(i=1,2)$ are constituted to realize the desired reaction force f_{dh} and also compensate the dynamic terms of the grip handle.

Using $\tilde{F}_{di}\,(i=1,2)$, we modify the tension feedback law as follows:

$$T_i=K_f(\tilde{F}_{di}-F_i)+F_{di} \quad (i=1,2). \quad (30)$$

By employing the above control law, we would be able to compensate the grip handle dynamics. However, it is difficult to calculate the modified desired wire tension $\tilde{F}_{di}$ from equations (28) and (29), because exact parameter values of the inertia m and the viscosity d, and exact signals of acceleration and velocity are difficult to obtain in practice.

To overcome this problem, we utilize the grip handle dynamics. Substituting equation (12) into equations (28) and (29), we obtain the following control law,

$$T_1=K_f\left\{F_{d1}-\frac{1}{2}(F_1+F_2-F_h)\right\}+F_{d1}, \quad (31)$$

https://doi.org/10.1017/S0263574798000551 Published online by Cambridge University Press

$$T_2 = K_f \left\{ F_{d2} - \frac{1}{2}(F_1 + F_2 + F_h) \right\} + F_{d2}, \tag{32}$$

where F_h can be measured by using an operational force sensor attached to the grip handle. We call the control law shown in equations (31) and (32) as the *tension and reaction force (T-RF) feedback law.* Using this control law, we will be able to compensate the grip handle dynamics without knowing its inertial and viscous coefficients.

Substituting equations (31) and (32) into equation (20), we obtain the following dynamics of the system under the T-RF feedback law,

$$N_K + \frac{1}{K}\{(m+2J)s^2 + (d+2D)s\}X = F_{dh} + F_h, \tag{33}$$

where the term N_K has been shown in equation (23). Thus,

$$F_\Delta = N_K + \frac{1}{K}\{(m+2J)s^2 + (d+2D)s\}X \tag{34}$$

is entirely dominated by K, namely the feedback gain K_f (because the term N_K is also dominated by K_f). Therefore, we can reduce the influence of F_Δ by setting high gain feedback and improve the structural transparency of the system. Effectiveness of the T-RF feedback law will be demonstrated in Section 9 through a basic experiment.

8.3 Stability analysis

Finally, we briefly discuss stability of the system under the T-RF feedback law. Similar to the analysis in Section 7, we have the following transfer function by setting the desired reaction force $F_{dh}=0$,

$$\tilde{G}_{FX} = \frac{X}{F_h}$$

$$= \frac{\frac{J}{K_0 K}s^2 + \frac{D}{K_0 K}s + 1}{\frac{Jm}{K_0 K}s^4 + \frac{Jd+Dm}{K_0 K}s^3 + \left(\frac{Dd}{K_0 K} + \frac{m+2J}{K}\right)s^2 + \frac{d+2D}{K}s} \tag{35}$$

$$= \frac{\frac{J}{K_0}s^2 + \frac{D}{K_0}s + K}{\frac{Jm}{K_0}s^4 + \frac{Jd+Dm}{K_0}s^3 + \left(\frac{Dd}{K_0} + m + 2J\right)s^2 + (d+2D)s}. \tag{36}$$

The corresponding plot of poles and zeros of $\tilde{G}_{FX}$ is shown in Figure 13, where the value of K is increased from 1 to 250. Since K does not appear in the denominator of the transfer function $\tilde{G}_{FX}$, positions of four poles are determined by the inherent dynamic characteristics of the system. On the other hand, two zeros will go to infinity in the left half of the complex number plane when the value of K is increased.

In the case of the T-RF feedback law, the system seems to be stable even if we choose any value for K, because all poles stay in the left half plane independently of the magnitude of K. However, the stability margin is determined from the inherent characteristics of the system and we cannot change this margin. Hence, we should choose the value of the feedback gain K_f carefully so that the unmodeled dynamics is not excited and it does not drive the system unstable.

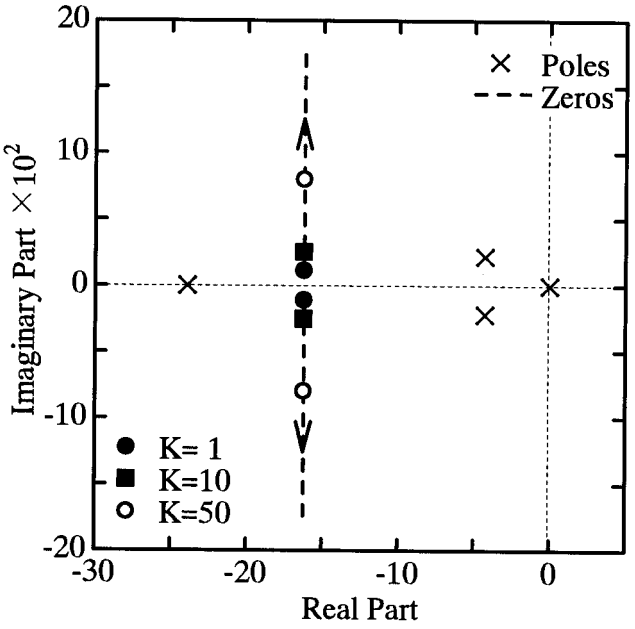


Fig. 13. Plot of poles and zeros of transfer function $\tilde{G}_{FX}$.

9. EXPERIMENTS

9.1 Experimental comparison of two control laws

We carried out a basic experiment for the force display system driven by parallel wire mechanism with two feedback control laws: the tension feedback law and the T-RF feedback law. The purposes of this experiment are

- to demonstrate validity of the T-RF feedback law for the structural transparency, compared to the tension feedback law, and
- to evaluate performance of the force display system driven by parallel wire mechanism quantitatively on the high speed motion capacity and the strucutral transparency.

We describe details of the experiment in the following.

9.1.1 Setup and procedure. Firstly, we set the desired reaction force $f_{dh}=0$. Then the operator grasped the grip handle of the system shown in Figure 4 and moved it downward as fast (namely, with a large velocity and a large acceleration) as possible. During an operation of the grip handle, we measured the grip handle position and the operational force. After the operation, we obtained a velocity and an acceleration of the grip handle by numerical differentiation. The experimental results were handled with a low pass filter whose cut off frequency is 40 [Hz], to demonstrate the results intelligibly. In this experiment, we

https://doi.org/10.1017/S0263574798000551 Published online by Cambridge University Press

set the same feedback gain to both control laws. The feedback gain K_f was chosen as 3.03 ($K=4.03$). It seems that a larger feedback gain could be chosen because the stability margin is enough from the analytical results shown in Figures 12 and 13. However, it was actually impossible because oscillation occurred on the force display system. It is presumed that the unmodeled dynamics of the force display system excites the oscillation.

9.1.2 Results. We examined each feedback law with the above procedure. The experimental results are shown in Figure 14. From this figure, we note that:

- In each acceleration trajectory, we observe two peaks. The former one means that the grip handle is accelerated, and the latter one does that the handle is decelerated.
- Each reaction force trajectory also has two peaks. Each peak corresponds to that in the acceleration trajectory. Here, a reaction force with a positive value means that an operator feels the force upward.

In the experimental results, we focused on the period in which the grip handle was accelerated (namely, the period until the velocity reached the maximum one from zero). In this period, we picked up peak values of velocities,

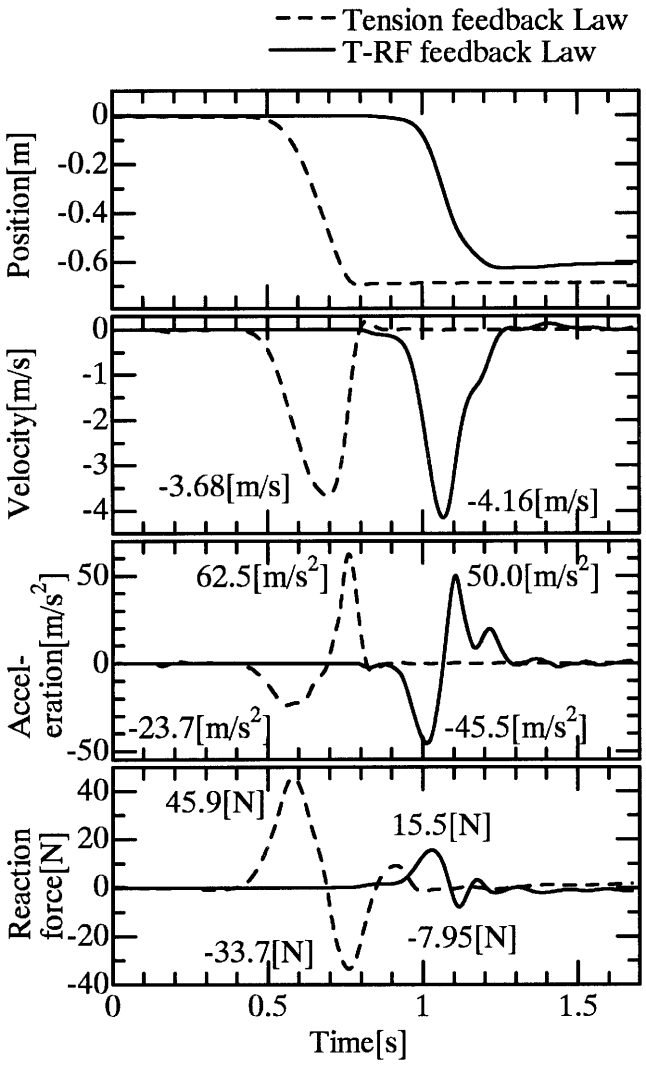


Fig. 14. Experimental results for feedback control laws.

Table III. Maximum (absolute) values of grip handle motion

Control law	Operated distance	Velocity [m/s]	Acceleration [m/s^2]	Reaction force [N]
Tension	0.689	3.68	23.7	45.9
T-RF	0.622	4.16	45.5	15.5
(Ratio)		(1.13)	(1.92)	(0.338)

acceleratons and reaction forces. Those values are shown in Table III, where each value is presented as an absolute one, and values inside parentheses denote ratios of the results in the case of the T-RF feedback law compared to those in the case of the tension feedback law.

9.1.3 Comparison and evaluation of results. Since we set the desired reaction force $f_{dh}=0$, the actual reacton force should also be zero from the ideal condition for the structural transparency given by equation (25) despite any motions of the grip handle. However, it will be actually impossible for any force display systems to satisfy the ideal condition. From a practical viewpoint, it is desirable that the force display system realizes a *higher* velocity and a *higher* acceleration with a *lower* reaction force.

Evaluating the results shown in Table III, we observed that a higher velocity and a higher acceleraton were realized with a lower reaction force when the T-RF feedback law was employed, compared to those when the tension feedback laws was used. From the result, we have verified that the structural transparency of the force display system driven by parallel wire mechanism is improved by using the T-RF feedback law.

Moreover, we apply another quantitative evaluation of the structural transparency for the experimental results. In this evaluation, we assume that the mechanical impedance of the whole system can be expressed as

$$M\ddot{x}+B\dot{x}+C_0\,\mathrm{sgn}(\dot{x})=f_h, \tag{37}$$

where, M, B and C_0 denote an effective inertial, viscous and coulomb frictional coefficients respectively. For each result shown in Figure 14, we calculate values of these coefficients by least squares method. The calculated values are summarized in Table IV.

In this evaluation, the ideal condition for the effective coefficients is $M=B=C_0=0$, because the ideal condition of $f_h=0$ should be satisfied for any motions of the grip handle. From a practical viewpoint, we can say that the force display system has higher structural transparency if all coefficients are relatively smaller (namely, the effective mechanical impedance is lower).

From Table IV, we know that all coefficients obtained

Table IV. Values of effective coefficients

Control law	M [kg]	B [kg/s]	C_0 [N]
Tension	0.771	2.96	1.44
T-RF	0.205	1.78	0.725

https://doi.org/10.1017/S0263574798000551 Published online by Cambridge University Press

from the result of the T-RF feedback law are smaller than those of the tension feedback law. That is, the T-RF feedback law has realized a lower mechanical impedance than that of the tension feedback law. Therefore, it is demonstrated that the T-RF feedback law is effective to improve the structural transparency of the force display system.

Through the results in Table IV, we know that our present 1 D.O.F. force display system driven by two wires has potential of realizing an effective mass of approximate 200 [g] while the actual mass of the grip handle is 500 [g]. The effective viscous and coulomb frinctional coefficients seems to be still large. It is presumed that such large coefficients are caused from the mechanical constraint using guide rails. In general parallel wire mechanisms with multiple degrees of freedom, such a mechanical constraint is unnecessary. Hence, it is expected that a multiple D.O.F. force display system driven by parallel wire mechanism realizes higher structural transparency with a smaller viscous and coulomb friction coefficients, as compared to those of the 1 D.O.F. system.

9.2 Force characteristic of system

We carried out a basic experiment to investigate the force characteristic of the system. In the experiment, we mechanically fixed the grip handle at $x=0$. Substituting $X=0$ to equation (22), we obtain the following transfer function

$$\frac{-F_h}{F_{dh}}=\frac{K_0K}{Js^2+Ds+K_0K}=\frac{\frac{K_0K}{J}}{s^2+\frac{D}{J}s+\frac{K_0K}{J}}. \tag{38}$$

From this equation, we know that

natural frequency: $$f_n=\frac{1}{2\pi}\sqrt{\frac{K_0K}{J}}, \tag{39}$$

damping factor: $$\zeta=\frac{D}{2\sqrt{K_0KJ}}. \tag{40}$$

In this experiment, we gave sinusoidal functions with various frequencies to the desired reaction force f_{dh}, and measured the actual reaction force-f_h for each frequency. As a result, the force characteristic of the system was obtained as a Bode diagram of transfer function $-F_h/F_{dh}$. The feedback gain is set as $K_f=3.03$ and thus $K=4.03$. We operated the system with three minimum wire tensions: $f_0=0.686$, 9.80 and 24.5 [N].

The experimental result is shown in Figure 15. The Bode diagram of the second order system was obtained. In this figure, we observe that by increasing the minimum wire tension, the peak of the gain moves to higher frequency. This means that the natural frequency f_n is increased by the minimum wire tension. The peak value of the gain is also raised, namely the damping factor is decreased by increasing the minimum wire tension.

The reason for these observations can be explained as follows: By increasing the minimum wire tension, the initial displacement a is increased. Therefore, the stiffness K_0 is also increased (recall the definition of K_0 given by equation (9)). Referring to equations (39) and (40), we consequently understand that increase on the stiffness K_0 yields increase on the natural frequency f_n and decrease on the damping factor ζ.

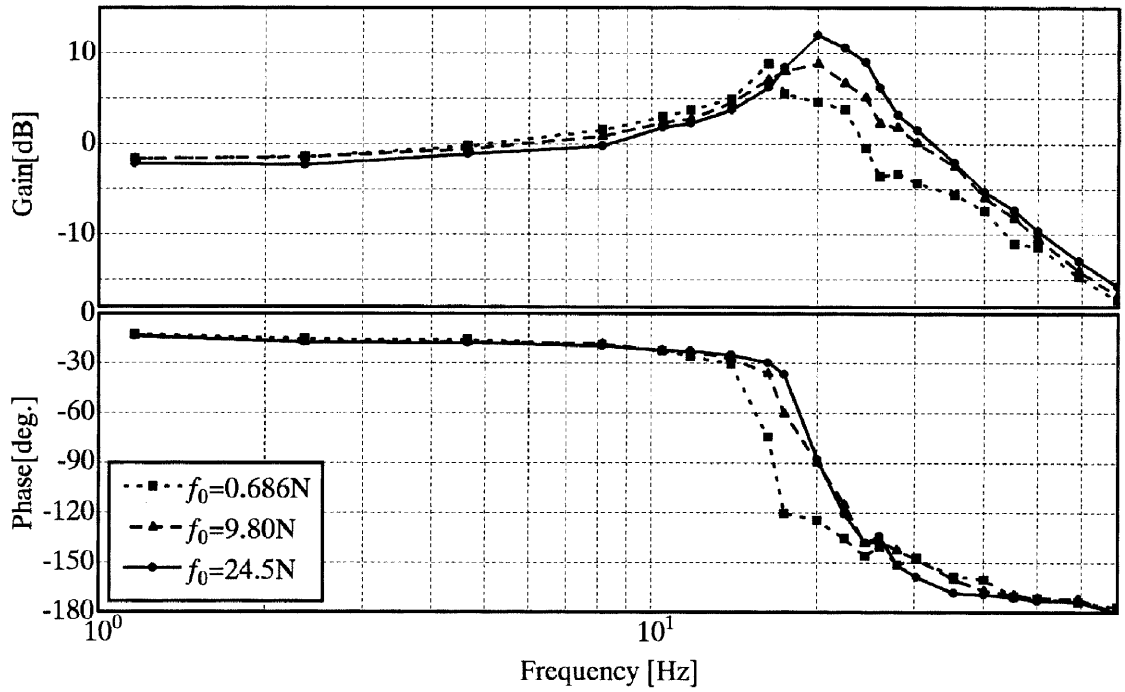


Fig. 15. Force characteristic of 1 D.O.F. system.

https://doi.org/10.1017/S0263574798000551 Published online by Cambridge University Press

10. CONCLUSION

In this paper, we have focused on the force display system driven by parallel wire mechanism, which has a potential to satisfy four characteristics of the large motion area, the high speed motion capacity, the operator's safety and the structural transparency. This type of force display system is essential in some applications of virtual reality, such as virtual sports training.

The main results of this paper are summarized as follows: Firstly, we have clarified the control issue of the force display system driven by parallel wire mechanism. The structural transparency of the system was affected by its both elastic characteristics of wires and motor units, and dynamics of the grip handle. Secondly, we have proposed control laws to reduce such effects and to improve the structural transparency. The tension feedback law could reduce the influence caused from the elasticity and the motor unit dynamics with a large feedback gain. However, this control law could not suppress the grip handle dynamics. To reduce this effect, we have proposed the tension and reaction force (T-RF) feedback law base on an idea of compensating the grip handle dynamics. The effectiveness of this control law has been demonstrated through the basic experiment. In addition, we have evaluated performance of the system using the experimental results.

As seen in equation (23), the elastic term N_K is inversely proportional to both the feedback gain K_f and the stiffness K_0. This stiffness can be increased by increasing the minimum wire tension, as shown in Section 9.2. From this consideration, we can also reduce influence of the elastic term N_K by employing a large wire tension to set the stiffness K_0 large.

In Section 4, we have seen that the assumption for the spring element was marginally satisfied for the 1 [Hz] motion of the grip handle. Referring to Figure 11(b), it seems that one way to validate the assumption for the motion with higher frequency is to set a larger wire tension to obtain a larger initial displacement so that minimum values of the displacement become positive. However, we should note that a problem of nonlinear oscillation might occur under such a large wire tension because the elasticity of the system is originally nonlinear.

We have seen in Section 9 that the effect of the unmodeled dynamics such as friction and non-linearity of the spring element is considerably large and hence limits the magnitude of the feedback gain. Therefore, such unmodeled dynamics should be analyzed as a future work.

References

1. K. Iwamoto and K. Tanie, "Binocular Head Mounted Display with Eye Movement Tracking Function – Development of the Prototype and Its Applicaton" *Proc. of the 1996 IEEE/RSJ Int. Conf. on Intelligent Robots and Systems*, Osaka (1996) pp. 354–359.
2. J.L. Wu, M. Nakahata and S. Kawamura, "A New Head Mounted Display System with Adjustable Disparity for High Depth-Performance" *Proc. of the 1995 IEEE Int. Conf. on Systems, Man and Cybernetics*, Vancouver (1995) pp. 298–303.
3. R. Hui and P. Gregorio, "The Virtual Handle" *Proc. of the 1995 IEEE/RSJ Int. Conf. on Intelligent Robots and Systems*, Pittsburgh (1995) pp. 127–132.
4. M. Ouh-young, M. Pique, J. Hughes, N. Srinivasan and F.P. Brooks, Jr, "Using A Manipulator For Forces Display In Molecular Docking" *Proc. of the 1988 IEEE Int. Conf. on Robotics and Automation*, Philadelphia (1988) pp. 1824–1829.
5. S. Shimizu, S. Ono, M. Sato, T. Odagawa, T. Izumi, M. Takahashi and T. Ifukube, "A basic Study of a Force Display using Metal Hydride Actuator" *Proc. of IEEE Int. Workshop on Robots and Human Communication*, (1993) pp. 211–215.
6. M. Otsuka, K. Kosuge, N. Matsumoto, T. Itoh and T. Idogaki, "Bilateral Telemanipulator System with Communication Time Delay Based on Force-Sum-Driven Virtual Internal Models" *Proc. of the 1995 IEEE Int. Conf. on Robotics and Automation*, Nagoya (1995) pp. 344–349.
7. Y. Yokokoji and T. Yoshikawa, "Bilateral Control of Master-Slave Manipulators for Ideal Kinesthetic Coupling" *Proc. of the 1990 IEEE/RSJ Int. Workshop on Intelligent Robots and Systems*, Tsuchiura (1990) pp. 355–362.
8. D.G. Caldwell, O. Kocak and U. Andersen, "Multi-armed Dexterous Manipulator Operation using Glove/Exoskeleton Control and Sensory Feedback" *Proc. of the 1995 IEEE/RSJ Int. Conf. on Intelligent Robots and Systems*, Pittsburgh (1995) pp. 567–572.
9. R.E. Ellis, O.M. Ismael and M.G. Lipsett, "Design and Evaluation of a High-Performance Haptic Interface" *Robotica*, **14**(3) (Vol. 14 Part 3) 321–327 (1996).
10. H. Kazerooni and G. Her, "A Virtual Exercise Machine" *Proc. of the 1993 IEEE Int. Conf. on Robotics and Automation*, Atlanta (1993) pp. 232–238.
11. R.D. Howe, "A Force Reflecting Teleoperated Hand System for the Study of Tactile Sensing in Precision Manipulation" *Proc. of the 1992 Int. Conf. on Robotics and Automation*, Nice (1992) pp. 1321–1326.
12. C.L. Collis and G.L. Long, "The Singularity Analysis of an In-Parallel Hand Controller for Force-Reflected Teleoperation" *IEEE Trans. on Robotics and Automation*, **11**(5), 661–669 (1995).
13. V. Hayward, "Toward a Seven Axis Haptic Device" *Proc. of the 1995 IEEE/RSJ Int. Conf. on Intelligent Robots and Systems*, Pittsburgh (1995) pp. 133–138.
14. S. Kawamura, W. Choe, S. Tanaka and S.R. Pandian, "Development of an Ultrahigh Speed Robot FALCON using Wire Drive System" *Proc. of the 1995 IEEE Int. Conf. on Robotics and Automation*, Nagoya (1995) pp. 215–220.
15. Y. Cai, M. Ishii and M. Sato, "A Human Interface Device for CAVE Size Virtual Workspace" *Proc. of the 1996 IEEE Int. Conf. on Systems, Man and Cybernetics*, Beijing (1996) pp. 2084–2089.
16. M. Ishii, M. Nakata and M. Sato, "Networked SPIDAR: A Networked Virtual Environment with Visual, Auditory, and Haptic Interactions" *Presence*, **3**(4), 351–359 (1994).
17. S. Kawamura and K. Ito, "A New Type of Master Robot for Teleoperation Using A Radial Wire Drive System" *Proc. of the 1993 IEEE/RSJ Int. Conf. on Intelligent Robots and Systems*, Yokohama (1993) pp. 55–60.
18. V.D. Nguyen, "Constructing Force-Closure Grasps in 3D", *Proc. of the 1987 IEEE Int. Conf. on Robotics and Automation*, (1987) pp. 240–245.
19. C. Melchiorri, M. Montanari and G. Vassura, "Control Strategies for a Defective, Wire-Based, Haptic Interface", *Proc. of the 1997 IEEE/RSJ Int. Conf. on Intelligent Robots and Systems*, Grenoble (1997) pp. 181–187.
20. S. Kawamura, M. Ida, T. Wada and J. L. Wu, "Development of A Virtual Sports Machine using A Wire Drive System – A Trial of Virtual Tennis –" *Proc. of the 1995 IEEE/RSJ Int. Conf. on Intelligent Robots and Systems*, Pittsburgh (1995) pp. 111–116.

https://doi.org/10.1017/S0263574798000551 Published online by Cambridge University Press